Materials Science & Engineering A 700 (2017) 250–258

Contents lists available at ScienceDirect

Materials Science & Engineering A

journal homepage: www.elsevier.com/locate/msea

Twinning and dynamic strain aging behavior during tensile deformation of Fe-Mn-C TWIP steel

Peng Lan*, Jiaquan Zhang*

School of Metallurgical and Ecological Engineering, University of Science and Technology Beijing, Beijing 100083, PR China

ARTICLE INFO

Keywords:
TWIP steel
Dynamic strain aging
Work hardening
Serrated flow
Local strain rate

ABSTRACT

The twinning and dynamic strain aging(DSA) induced work hardening in Fe-Mn-C TWIP steel has been experimentally investigated in view of grain morphology, stress strain response, local strain rate(LSR) and strain hardening rate. A strain of 0.3 should be the critical value for the saturation of twined grains in Fe-Mn-C TWIP steel with 0.4–0.6 wt% carbon and 18–22 wt% manganese. DSA can occur in the very beginning of plastic deformation in Fe-Mn-C TWIP steel with the unpronounced fluctuation in stress strain response but obvious discontinuity in work hardening and LSR. The mechanism on strain hardening of Fe-Mn-C TWIP steel during tensile deformation can be distinguished by the variation of LSR. Twinning induced hardening rate is around 3.0 GPa with a steady LSR, while DSA induced hardening rate is about 2.0 GPa with a periodic and unstable fluctuation of LSR. There are mainly three stages in the work hardening of Fe-Mn-C TWIP steel divided by the inducing mechanism: twinning dominant, twinning + DSA dominant and DSA dominant. A strong correlation between the fluctuating characteristic of LSR and work hardening rate has been observed. In twinning dominant stage, they are largely steady; while in the other two stages, more significant fluctuation is observed where DSA is more pronounced for both curves. The serration in stress corresponds to the plateau in strain and low LSR, as well as the peak of strain hardening rate, due to the occurrence of DSA; and the smooth stress evolution between two serrations correlates the apparent increase of strain, and high LSR, together with the trough of strain hardening rate, relating to the preparation time for next DSA.

1. Introduction

Twinning induced plasticity(TWIP) steel has been regarded as a potential candidate for the lightweighting of automobiles, attributed to the high work hardening property and high energy absorption performance. The application of TWIP steel in the manufacture of car body components leads to the decrease of fuel consumption and exhaust emission without the drop of crashing safety. In recent years, TWIP steel has been drawn much attention due to the excellent combination of high strength, ductility and formability [1–3]. The investigations on the composition design, microstructure control, property enhancement and deformation mechanism have been widely reported [4–7].

Grassel and Frommeyer introduced a high manganese steel in Fe-(15 − 30)Mn-(2 − 4)Si-(2 − 4)Al system about 20 years ago [8,9]. The tensile strength and total elongation under the strain rate from $10^{-4}\,s^{-1}$ to $10^{3}\,s^{-1}$ reached 600–900 MPa and 60–90% respectively. Twinning behavior was supposed as the deformation mechanism for this first generation of TWIP steel. Scott and Allain designed a new type of TWIP steel in Fe-Mn-C system [10,11]. The tensile strength increased to 1000 MPa and the elongation decreased to 50% approximately. Secondary twins and serrated flow, which were absent in the Fe-25Mn-3Si-3Al TWIP steel, were clearly observed in the deformed matrix of Fe-22Mn-0.6C steel. Delayed fracture, associated with hydrogen segregation, ε-martensite transformation, and twinning intersection, has been experimentally confirmed in Fe-Mn-C TWIP steel recently [12–14]. Accordingly, a new TWIP steel in the composition of Fe-18Mn-0.6C-(1.5–2.0)Al was commercially developed with the concept that Al addition is an effective solution to delayed fracture [15,16]. The second generation TWIP steel in Fe-Mn-C(-Al) system, with twinning and dynamic strain aging(DSA) induced strain hardening performance, has been widely studied. Barbier and Gey experimentally analyzed the texture and microstructure evolution during tensile process of Fe-22Mn-0.6C TWIP steel, and the prevention of dislocation movement by primary and secondary twins was proposed as the strengthening mechanism [17]. Gutierrez-Urrutia and Raabe investigated the deformation behavior of TWIP steel with similar composition by electron channeling contrast imaging, and the interaction between dislocation and twin substructure was regarded to be the factor influencing work

* Corresponding authors.
E-mail addresses: lanpeng@ustb.edu.cn (P. Lan), jqzhang@metall.ustb.edu.cn (J. Zhang).

http://dx.doi.org/10.1016/j.msea.2017.06.012
Received 10 March 2017; Received in revised form 2 June 2017; Accepted 3 June 2017
Available online 06 June 2017
0921-5093/

hardening [18]. Another important phenomenon, the DSA behavior, has also been an attractive topic in the field of high interstitial-contained TWIP steel. Dastur and Leslie argued that twinning was not the major contribution for the high work hardening rate of high Mn steel [19]. Hong and Shin studied the DSA of Fe-22Mn-0.6C TWIP steel by observing Portevin-Le Chatelier(PLC) bands and the corresponding serrated flow [20]. They found that the stress/strain concentration happened within PLC bands due to the interaction between C-Mn point defect complex and stacking fault. Chen [21] and Zavattieri [22] carried out a similar research on PLC bands in Fe-Mn-C TWIP steel respectively, and some parameters such as band moving velocity, band width and band angle et al. were mathematically discussed. Lee and Kim investigated the origin of DSA in Fe-Mn-C and Fe-Mn-C-Al TWIP steel by both theoretical and experimental method [23]. They addressed that DSA occurred by a single diffusive jump of the C atom of the point defect complex in the stacking fault region, which can be only observed when the C atom reorientation time was smaller than the residence time of the stacking fault at the location of the point defect complex.

It has been commonly accepted that both twinning and DSA are the major contribution for the excellent work hardening of high C-contained TWIP steel [24]. Chen and Kim analyzed the stress-strain response and work hardening performance of Fe-18Mn-0.6C TWIP steel. They pointed out that twinning induced strengthening was not that pronounced, which was dominant just in a short stage before the onset of DSA [21]. Saeed-Akbari and Mishra studied the dislocation planar glide, twinning and DSA in Fe-Mn-C TWIP steels. They proposed a competition mechanism for work hardening in different strain range [25,26]. Koyama and Sawaguchi distinguished the work hardening rate in different mechanism by a tensile test with Fe-17Mn-0.6C and Fe-17Mn-0.8C steels. It was found that the work hardening rate was about 4 GPa attributed from martensite transformation, while 3 GPa and 2.3 GPa from deformation twinning and DSA respectively [27]. The present author also carried out some investigations on the solidification microstructure, hot ductility, and mechanical performance of TWIP steel [1,28–33]. According to our previous research [31,33], twinning and DSA take effect simultaneously during tensile deformation of Fe-Mn-C TWIP steel. The study focusing on separate phenomenon cannot elaborate the integrated behavior clearly. The present study is aiming to make a clear description on the deformation behavior of Fe-Mn-C TWIP steel and elucidate the mechanism of strain hardening. Both twinning and DSA in Fe-(20,22,24)Mn-(0.4,0.6)C TWIP steel was investigated on basis of experimental observation. It is shown that the dominant hardening mechanism in Fe-Mn-C TWIP steel can be distinguished well by the comparison of local strain rate(LSR) and strain hardening rate.

2. Materials and experiment

Four Fe-Mn-C steels were cast with 25 kg vacuum medium frequency induction melting furnace. The measured compositions were shown in Table 1, together with stacking fault energy by two sublattice method [32,33]. The concentration of C and S was measured through infrared absorptiometric method after combustion in current oxygen, and Mn content was determined by perchloric acid oxidation trivalent manganese titrimetric method. In addition, inert gas carrier melting thermo-conductimetric method was employed for the measurement N concentration, while inert gas carrier melting infrared absorptiometric method was introduced for measuring O. The contents of other alloying elements (Si, Al and P) were measured by ICP-OES (Inductively coupled plasma optical emission spectrometric) methodology.

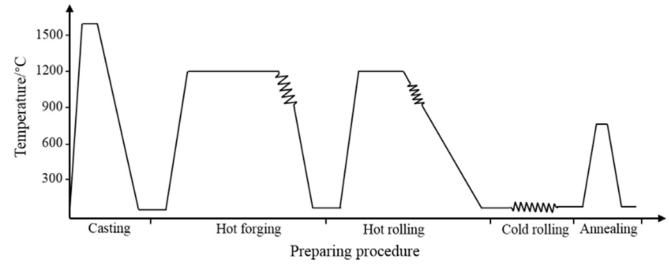

Fig. 1. Preparing procedure of TWIP steel samples.

The material preparation process is schematically presented in Fig. 1. The as cast ingots of TWIP steel with 120 mm in diameter and 250 mm (excluding hot-top) in height were heated to 1200 °C and soaked for 2 h by box-type muffle furnace, then forged into rectangular bars sized about 30 mm × 80 mm × 1000 mm. The finishing temperature was higher than 900 °C, and the hot forged samples were cooled to room temperature by air convection. Hot rolling was carried out on hot forged samples by a double roller machine at 1100 °C after soaking at 1200 °C for 1 h. After five passes, the forged bars were rolled to plates with thickness between 3.9–4.0 mm, then the samples with temperatures higher than 900 °C were cooled in furnace. Cold rolled was operated after pickling by aqueous hydrochloric acid solution at room temperature. The final sheets were about 1.6 mm in thickness after ten passes with the total reduction rate about 60%. Finally, the sheet samples were heat treated at 750 °C for 10 min, then air-cooled to 25 °C. According to ASTM E8M-13a, the sub-size tensile samples with the gauge of 25 mm × 6 mm were prepared, as shown in Fig. 2. The uniaxial tensile test was conducted with CMT5105 electric universal testing machine at a constant strain rate of 10^{-3} s^{-1}, while the measure range of electric extensometer during deformation was 0–100%. The deformation microstructure of TWIP steel was observed by Olympus Lext OLS4000 optical microscope(OM) and FEI MLA250 scanning electronic microscope(SEM) after mechanical polishing and chemical etching by Nital. MAC Science M21X ultrahigh power X-ray diffractometer was employed to examine the phase transformation before and after deformation. The detected surface of the sample was gently grinded and chemically polished(H_2O_2:HF = 10:1). The acceleration voltage was 40 kV and the scanning rate was 5°/min with a Cu target.

3. Results

3.1. Matrix phase evolution

Fig. 3 shows the XRD results for different samples before and after tensile test. It can be seen that the matrix phase of TWIP steel after annealing is fully austenite for all samples in Fe-Mn-C system, as shown in Fig. 3(a). After tensile-deformed to fracture, a little HCP martensite was detected in 1# sample while single austenite matrix was confirmed for others, as shown in Fig. 3(b). Based on our previous research [32,33], the SFE calculated by two sublattice model is 14.0 mJ/m^2 for 1# sample, but SFEs for others are higher than 18 mJ/m^2. According to

Table 1
Chemical composition of investigated steels, wt%.

	C	Si	Mn	P	S	Al	T.O	T.N	SFE, mJ mol^{-1}
1#	0.46	0.17	19.74	0.005	0.005	< 0.005	0.0017	0.0050	14.0
2#	0.42	0.18	22.28	0.004	0.003	< 0.005	0.0023	0.0037	19.4
3#	0.61	0.17	20.08	0.005	0.004	< 0.005	0.0020	0.0053	20.4
4#	0.60	0.19	23.77	0.005	0.004	< 0.005	0.0025	0.0044	33.5